

# Hints of correlation between broad-line and radio variations for 3C 120

H. T. Liu<sup>1,2</sup>, J. M. Bai<sup>1,2</sup>, J. M. Wang<sup>3,4</sup> and S. K. Li<sup>1,2</sup>  
htliu@ynao.ac.cn

## ABSTRACT

In the paper, we investigate correlation between broad-line and radio variations for broad-line radio galaxy 3C 120. By the  $z$ -transformed discrete correlation function method and the model-independent flux randomization/random subset selection (FR/RSS) Monte Carlo method, we find that the broad  $H\beta$  line variations lead the 15 GHz variations. The FR/RSS method shows that the  $H\beta$  line variations lead the radio variations by a factor of  $\tau_{\text{ob}} = 0.34 \pm 0.01$  yr. This time lag can be used to locate the position of emitting region of radio outbursts in jet, on the order of  $\sim 5$  light-years, from the central engine. This distance is much larger than the size of broad-line region. The large separation of the radio outburst emitting region from the broad-line region will observably influence the gamma-ray emission in 3C 120.

*Subject headings:* galaxies: active – galaxies: individual (3C 120) – galaxies: jets – quasars: emission lines – radio continuum: galaxies

## 1. INTRODUCTION

According to the reverberation mapping model (e.g. Blandford & McKee 1982), the broad emission line variations follow the ionizing continuum variations through the photoionization process. The variation correlations between broad-lines and continua were observed with time lags in type 1 active galactic nuclei (AGNs, see e.g. Kaspi & Netzer 1999; Kaspi et al. 2000; Peterson et al. 2005). The disturbances from the central engine in AGNs are transported with ionizing continua to broad-lines. Theoretical researches show that the jets can be ejected from inner accretion disk in the vicinity of the central black hole (e.g. Penrose 1969; Blandford & Znajek 1977;

Blandford & Payne 1982; Meier et al. 2001). Rawlings & Saunders (1991) indicated a disk-jet symbiosis with comparable power channelled through the disk and the jet. Correlations between radio powers and broad-line luminosities are found for AGNs and are regarded as evidence for the disk-jet symbiosis (see e.g. Celotti et al. 1997; Cao & Jiang 1999, 2001; Wang et al. 2003; Liu & Bai 2010). These previous results indicate that the disturbances in the central engine are likely propagated outwards along the jets. Observations show that dips in the X-ray emission, generated in the central engine, are followed by ejections of bright superluminal radio knots in the jets of AGNs and microquasars (e.g. Marscher et al. 2002; Arshakian et al. 2010). The dips in the X-ray emission are well correlated with the ejections of bright superluminal knots in the radio jets of 3C 120 (Chatterjee et al. 2009) and 3C 111 (Chatterjee et al. 2011). The outbursts are physically linked to the ejections of superluminal knots (e.g. Türler et al. 2000). Then these outbursts of broad-line and jet emission might respond to the stronger disturbances in the central engine. It is expected that there might be correla-

<sup>1</sup>Yunnan Observatories, Chinese Academy of Sciences, Kunming, Yunnan 650011, China

<sup>2</sup>Key Laboratory for the Structure and Evolution of Celestial Objects, Chinese Academy of Sciences, Kunming, Yunnan 650011, China

<sup>3</sup>Key Laboratory for Particle Astrophysics, Institute of High Energy Physics, Chinese Academy of Sciences, 19B Yuquan Road, Beijing 100049, China

<sup>4</sup>Theoretical Physics Center for Science Facilities, Chinese Academy of Sciences, Beijing 100049, China

tions with time lags between variations of broad-line and jet emission. A method was proposed to connect the time lags, the size of broad-line region (BLR), and the location of jet emission for blazar 3C 273 (Liu et al. 2011a, hereafter Paper I).

The BLRs are important to gamma-ray emission in blazars. The gamma rays from blazars are generally believed to be from a relativistic jet with a small viewing angle (Blandford & Rees 1978). The diffuse radiation field of BLR could have a strong impact on the expected external Compton (EC) spectrum of the most powerful blazars (see e.g. Sikora et al. 1994; Wang 2000; Liu & Bai 2006; Reimer 2007; Liu et al. 2008; Sitarek & Bednarek 2008; Tavecchio & Ghisellini 2008; Bai et al. 2009; Tavecchio & Mazin 2009). This strong impact rises from two factors. One of them is the seed photons from the BLR in the inverse Compton scattering, and the seed photons significantly influence the EC spectrum. The other is photon-photon absorption between the seed photons and the gamma-ray photons of the EC spectrum. There is a underlying physical factor that constrains how much the above two factors influence on the gamma-ray spectrum. The underlying factor is the location of gamma-ray-emitting region relative to the BLR. If the gamma-ray-emitting region is inside the BLR, the gamma-ray spectrum will shift to higher energies and the gamma-ray luminosity will become larger due to the relativistic effects. At the same time, the photon-photon absorption becomes more significant as the emitting region goes deeper into the BLR (see Liu & Bai 2006; Liu et al. 2008; Bai et al. 2009). As the emitting region is outside the BLR, the gamma-ray spectrum will shift to lower energies and the gamma-ray luminosity will become lower due to the relativistic effects. At the same time, the photon-photon absorption becomes insignificant as the emitting region keeps away from the BLR. Thus it is valuable to connect the BLR size with the location of jet emission. It will be an important step for this connection to confirm correlation between variations of broad-lines and radio emission of jet and to estimate the relevant time lags. In the paper, we study this issue in the broad-line radio galaxy 3C 120.

The structure of this paper is as follows. Section 2 presents method. Section 3 presents application to 3C 120. Section 3 contains three subsections:

subsection 3.1 presents constraint on time lag, subsection 3.2 data of 3C 120, and subsection 3.3 analysis of time lag. Section 4 is for discussion and conclusions. In this work, we assume the standard  $\Lambda$ CDM cosmology with  $H_0 = 70 \text{ km s}^{-1} \text{ Mpc}^{-1}$ ,  $\Omega_M = 0.27$ , and  $\Omega_\Lambda = 0.73$ .

## 2. METHOD

According to equation (7) in Paper I, we have a relation between  $R_{\text{BLR}}$ ,  $R_{\text{radio}}$ , and  $\tau_{\text{ob}}$

$$R_{\text{BLR}} = R_{\text{radio}} \left( \frac{c}{v_d} - \cos\theta \right) - \frac{c\langle\tau_{\text{ob}}\rangle}{1+z}, \quad (1)$$

where  $R_{\text{BLR}}$  is the size of the BLR,  $R_{\text{radio}}$  is the radio-emitting location of the jet,  $c$  is the speed of light,  $v_d$  is the travelling speed of disturbances down the jet, equivalent to the bulk velocity of jet  $v_j$ ,  $\theta$  is the viewing angle of the jet axis to the line of sight, and  $\langle\tau_{\text{ob}}\rangle \equiv \tau_{\text{ob}}$  is the measured time lag of the radio emission relative to the broad lines. From the velocity  $\beta = v_j/c$  and the viewing angle  $\theta$ , we have the apparent speed  $\beta_a = \beta\sin\theta/(1 - \beta\cos\theta)$ , which gives  $\beta = \beta_a/(\beta_a\cos\theta + \sin\theta)$ . Substituting this expression of  $\beta$  for the velocity term in equation (1), we have

$$R_{\text{BLR}} = R_{\text{radio}} \frac{\sin\theta}{\beta_a} - \frac{c\langle\tau_{\text{ob}}\rangle}{1+z}. \quad (2)$$

From equation (2), we have an expression to estimate  $\langle\tau_{\text{ob}}\rangle$

$$\langle\tau_{\text{ob}}\rangle = \left( R_{\text{radio}} \frac{\sin\theta}{\beta_a} - R_{\text{BLR}} \right) \frac{1+z}{c}. \quad (3)$$

## 3. APPLICATION TO 3C 120

3C 120, at redshift  $z = 0.033$ , has the one-sided jet with the apparent superluminal motion in the approaching jet (Gómez et al. 2001). The central supermassive black hole of this object has a mass of a few times  $10^7 M_\odot$  (Peterson et al. 1998a, 2004).

### 3.1. Constraint on time lag

The Very Long Baseline Array (VLBA) imaging observations revealed a very complex radio jet in 3C 120, such as superluminal components, stationary components, and trailing components in inner jet (Gómez et al. 2001; Jorstad et al.

2005; Chatterjee et al. 2009; León-Tavares et al. 2010). There are two stationary features in the radio jet, D and S1 (León-Tavares et al. 2010). The feature D is located at the base of the jet, and could be the core of the jet. The feature S1 is most likely a standing shock formed in the jet. As the moving knots pass through the stationary feature S1, these knots will produce outbursts. The process was tested in the optical light curves of 3C 120 with peaks corresponding to the moving component passages through S1. It is not possible to verify whether the radio flux density reacted to the passage of moving features in the same fashion as the optical continuum. The prominent superluminal feature o reaches its maximum flux density around 0.5 mas from the radio core (Gómez et al. 2001). The stationary feature S1 was identified at  $\sim 0.7$  mas separated from the VLBA 43 GHz core (León-Tavares et al. 2010). Thus the radio outbursts may originate in the region from D to S1 in the inner jet.

For 3C 120, Chatterjee et al. (2009) derived a distance of  $\sim 0.5$  pc from the corona to the VLBA 43 GHz core region using the average time delay between the start of the X-ray dips and the time of ejection of the corresponding superluminal knots. For 3C 111, a distance of  $\sim 0.6$  pc from the corona is estimated with the same method as in 3C 120 (Chatterjee et al. 2011). The 43 GHz VLBA observations give the global parameters of the jet for 3C 120, such as  $\theta = 20.5 \pm 1.8^\circ$  (Jorstad et al. 2005). These global parameters are widely accepted by other researchers. The 15 GHz components may correspond to the strongest events in the central engine (León-Tavares et al. 2010). Due to the optical depth, the 15 GHz outburst may follow the 43 GHz outburst. The emitting location of the 15 GHz outburst is estimated as the sum of the distance of 0.5 pc from the corona to the VLBA core and the de-projected distance of 0.0–0.7 mas from the VLBA core. Under the standard  $\Lambda$ CDM cosmology we considered, an angular separation of 1 mas in the sky corresponds to a projected linear distance of 0.66 pc. The de-projected distance of 0.7 mas from the radio core is equal to  $0.7 \times 0.66 \text{ pc} / \sin\theta = 0.7 \times 0.66 \text{ pc} / \sin 20.5^\circ = 1.32 \text{ pc}$ . The distance of 15 GHz outburst emitting region from the central engine is  $R_{\text{radio}} \sim 0.5 \text{ pc} - 0.5 \text{ pc} + 1.32 \text{ pc} = 0.5 - 1.82 \text{ pc} = 1.63 - 5.93 \text{ ly}$ . For 3C 120, the  $H\beta$  line has a BLR

size of  $R_{\text{BLR}} = 43.8_{-20.3}^{+27.7}$  light-days, i.e.  $R_{\text{BLR}} = 0.12_{-0.06}^{+0.08}$  ly (Peterson et al. 1998a). The apparent speeds of the moving components with well-determined motions are all within a range of  $\beta_a = 4.0 \pm 0.2$  (Chatterjee et al. 2009). Based on equation (3),  $R_{\text{BLR}} = 0.12 \text{ ly}$ ,  $\beta_a = 4.0$ ,  $\theta = 20.5^\circ$  and  $R_{\text{radio}} = 1.63 - 5.93 \text{ ly}$ , we derive  $\tau_{\text{ob}} > 0$ . This positive time lag means that the broad-line variations lead the radio variations.

### 3.2. Data of 3C 120

We make use of the 15 GHz light curve with a higher sampling rate of 59 times per year. This radio light curve is published in Richards et al. (2011). For the  $H\beta$  line, Nuñez et al. (2012) presents a light curve with a very dense sampling of 20 times per month, and also Grier et al. (2012) presents a light curve of sampling 20 times per month in the reverberation mapping observations. These light curves are presented in Figure 1, and are used to analyze the cross-correlation between them.

### 3.3. Analysis of Time Lag

The z-transformed discrete correlation function (ZDCF; Alexander 1997) is used to analyze time lags characterized by the centroid of the ZDCF. The ZDCF method is straightforward to determine whether there is a time lag between different light curves, and firstly it is applied to analyze the time lags. The centroid time lag  $\tau_{\text{cent}}$  is computed by all the points with correlation coefficients not less than 0.8 times the maximum of correlation coefficients in the ZDCF bumps closer to the zero-lag. The uncertainties of each point in the ZDCF only take into account the uncertainties from the measurements by Monte Carlo simulation, and the uncertainties of time lags are underestimated (see Liu et al. 2011b, hereafter Paper II). Thus we use the model-independent flux randomization/random subset selection (FR/RSS) Monte Carlo method (Peterson et al. 1998b) to re-estimate the time lags and their uncertainties in the cross-correlation results. The FR/RSS method is based on the discrete correlation function (DCF) method (Edelson & Krolik 1988) for the sparsely sampled light curves, and on the interpolated cross-correlation function (ICCF) method for the densely sampled light curves.

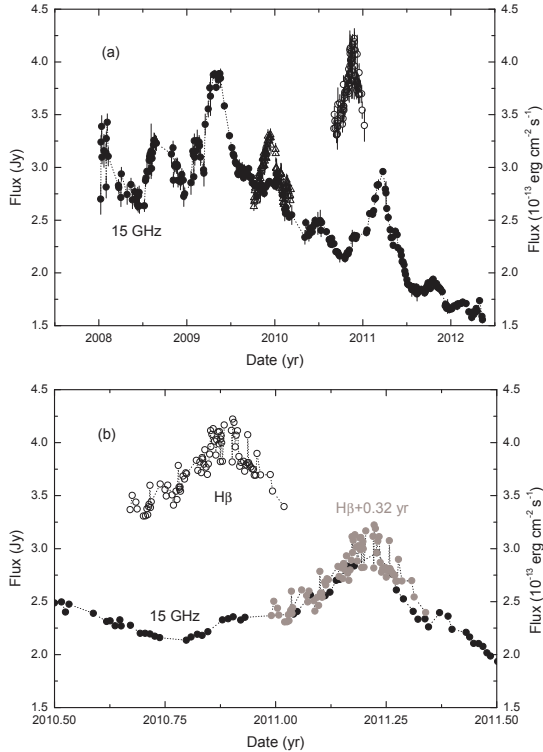


Fig. 1.— Light curves of  $H\beta$  and 15 GHz emission. Black open triangles denote the  $H\beta$  light curve of Nuñez et al (2012). Black open circles denote the  $H\beta$  light curve of Grier et al. (2012). Black solid circles denote the 15 GHz light curves in units of Jy. The  $H\beta$  line is in units of  $10^{-13}$  erg  $\text{cm}^{-2}$   $\text{s}^{-1}$ . Gray solid circles denote the  $H\beta$  light curve moved along the  $x$ - and  $y$ -axes.

The  $H\beta$  line light curves with a very dense sampling are published in 2012 (Grier et al. 2012; Nuñez et al 2012). 3C 120 is densely observed from 2008.0 to 2012.5 in the 15 GHz radio monitoring program with the 40 m telescope at the Owens Valley Radio Observatory (Richards et al. 2011). Firstly, it is obvious that the  $H\beta$  line light curve in Grier et al. (2012) can be well matched with the outburst in the 15 GHz light curve from 2011.0 to 2011.3 as the line light curve is moved right by 0.32 yr (see Figure 1b). The ZDCF method and the FR/RSS method are performed to investigate the correlation between these  $H\beta$  line light curves and the 15 GHz light curve, and estimate the time lags from the correlation. As these two line light curves are combined into one light curve, the calculated ZDCF is presented in Figure 2a. The horizontal and vertical error bars in Figure 2a represent the 68.3 per cent confidence intervals in the time lags and the relevant correlation coefficients, respectively. There are positive and negative correlations (see Figure 2a). The positive correlation has a time lag around 0.3 yr. The  $H\beta$  line variations lead the 15 GHz variations by a factor of  $\sim 0.3$  yr. This lag has the same sign as that lag estimated in section 3.1. This indicates that the positive correlation is reliable. For the positive correlation, the ZDCF method gives  $\tau_{\text{cent}} = 0.305^{+0.011}_{-0.002}$  yr. The FR/RSS method gives  $\tau_{\text{cent}} = 0.336^{+0.012}_{-0.010}$  yr with a mean of peak correlation coefficients  $r = 0.59 \pm 0.07$  in Monte Carlo simulations of 10,000 runs (see Figure 2b). This time lag is well consistent with that lag derived from the ZDCF method.

The 15 GHz light curve shows a simple baseline superimposed with some outbursts and flares (see Figure 3a). This baseline should influence the cross-correlation function between this radio light curve and the  $H\beta$  line light curve. Thus we subtract this baseline assumed as a simple gaussian profile from the 15 GHz light curve. It is obvious that the simple gaussian profile can well account for the underlying baseline in the 15 GHz light curve (see Figure 3a). The cross-correlation function between the residual radio light curve and the  $H\beta$  line light curve is calculated with the ZDCF method and the FR/RSS method. The calculated ZDCF is presented in Figure 3b. The positive cross-correlation around 0.3 yr is re-confirmed, and the significance of cross-correlation is signif-

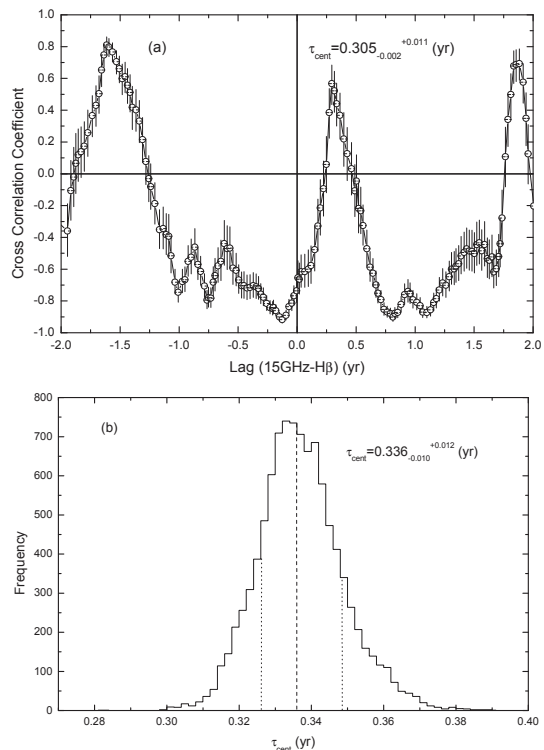


Fig. 2.— (a) ZDCF between the H $\beta$  and 15 GHz light curves. (b) Distribution of  $\tau_{\text{cent}}$  obtained with the FR/RSS method. The vertical dashed line is the median of distribution, and the dotted lines show the 68.3 per cent confidence interval of  $\tau_{\text{cent}}$ .

icantly improved with this residual light curve. The ZDCF method gives  $\tau_{\text{cent}} = 0.328_{-0.004}^{+0.014}$  yr. The FR/RSS method gives  $\tau_{\text{cent}} = 0.34 \pm 0.01$  yr with a mean of peak correlation coefficients  $r = 0.88 \pm 0.02$  in Monte Carlo simulations of 10,000 runs (see Figure 3c). This time lag is in excellent agreement with that lag derived from the ZDCF method. The broad H $\beta$  line variations lead the 15 GHz variations. Hereafter,  $\tau_{\text{cent}}$  is equivalent to  $\tau_{\text{ob}}$ .

#### 4. DISCUSSION AND CONCLUSIONS

We simplify the ionizing continuum region to be a point. This simplification indicates that the disturbances will simultaneously be transported outwards with the ionizing continuum and the relativistic jet, i.e. it makes equations (1)–(3) to be valid. This simplification will influence the time lag  $\tau_{\text{ob}}$ . The disturbances in the accretion disk will take a certain time to travel between their location of origin and the event horizon of the central black hole. Then the disturbances will take some time to pass through the ionizing continuum region to the event horizon. For 3C 120, the UV ionizing continuum region is located at  $\sim 5r_g$  from the black hole, where  $r_g = GM_{\text{BH}}/c^2$  is the gravitational radius of the black hole (Chatterjee et al. 2009). The black hole mass is on the order of  $10^7 M_{\odot}$  (Peterson et al. 1998a, 2004), and the size of  $\sim 5r_g$  is on the order of  $10^{-5}$  ly. If the disturbances are a thermal fluctuation propagating inward, it should have an effective speed  $\lesssim 0.01c$  (Chatterjee et al. 2009), to cause a time delay of  $\gtrsim 0.001$  yr for the distance of  $\sim 5r_g$ . This time delay should be negligible compared with the time lag  $\tau_{\text{ob}} = 0.34$  yr. In estimation of the magnitude of  $\tau_{\text{ob}}$  in section 3.1, we use the distance of  $\sim 0.5$  pc from the VLBA 43 GHz core region to the corona in the accretion disk-corona system, and ignore the size of corona. The size of corona may influence  $\tau_{\text{ob}}$ . The coronal radius is  $\sim 40r_g$  (Chatterjee et al. 2009). The jet velocity near the central engine will be  $\sim 0.9c$  (see Paper I), and this radius of  $\sim 40r_g$  will cause a time delay on the order of  $10^{-4}$  yr. The time delay is negligible.

From equation (2), we have an expression to estimate  $R_{\text{radio}}$  from  $\beta_a$ ,  $\theta$ ,  $R_{\text{BLR}}$  and  $\tau_{\text{ob}}$

$$R_{\text{radio}} = \frac{\beta_a}{\sin \theta} \left( R_{\text{BLR}} + \frac{c \langle \tau_{\text{ob}} \rangle}{1+z} \right). \quad (4)$$

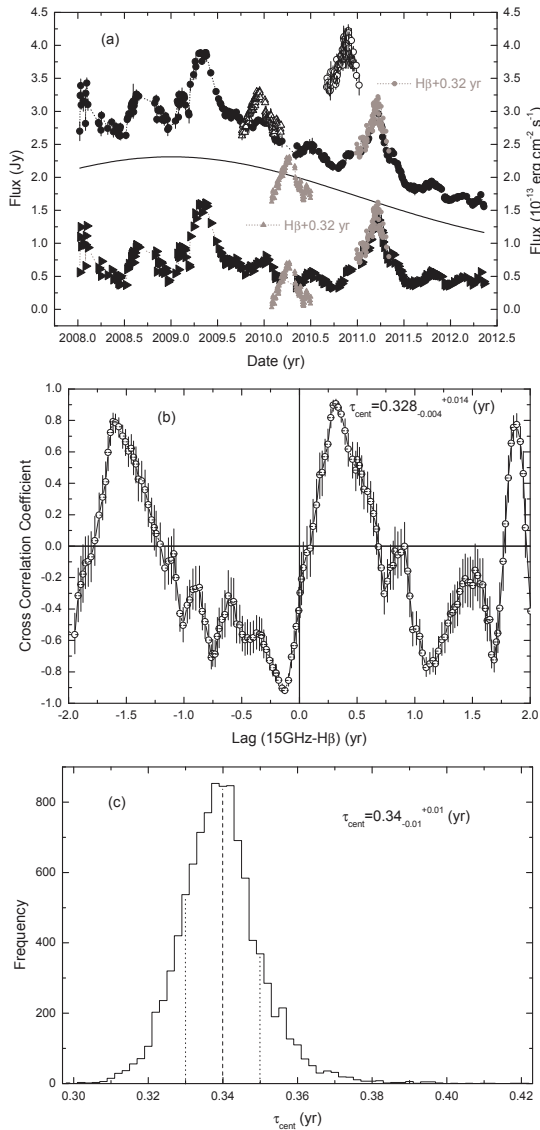


Fig. 3.— (a) Comparison between the 15 GHz and  $H\beta$  light curves. Black right triangles are the 15 GHz light curve subtracted by a assumed simple baseline denoted with the black solid line. Gray symbols are the  $H\beta$  light curve moved along the  $x$ - and  $y$ -axes. Other symbols are same as in Figure 1. (b) ZDCF between the modified 15 GHz light curve and the  $H\beta$  light curve in black color. (c) Distribution of  $\tau_{\text{cent}}$  obtained with the FR/RSS method. The vertical dashed and dotted lines are same as in Figure 2b.

For  $\beta_a = 4.0 \pm 0.2$ ,  $\theta = 20.5 \pm 1.8^\circ$ ,  $R_{\text{BLR}} = 0.12^{+0.08}_{-0.06}$  ly, and  $\tau_{\text{ob}} = 0.34 \pm 0.01$  yr, we have  $R_{\text{radio}} = 5.24 \pm 0.16$  ly from Monte Carlo simulations based on equation (4). Thus we have  $R_{\text{BLR}} \ll R_{\text{radio}}$  for 3C 120. *Fermi*-Large Area Telescope (LAT) detected gamma rays from 3C 120 (Kataoka et al. 2011), and it was suggested that the GeV emission of broad-line radio galaxies is most likely dominated by the beamed radiation of relativistic jets observed at intermediate viewing angles. The radio and gamma-ray emitting regions are closely connected with each other, and there is  $R_\gamma \lesssim R_{\text{radio}}$  between the radio-emitting position  $R_{\text{radio}}$  and the gamma-ray-emitting location  $R_\gamma$  (e.g., Dermer & Schlickeiser 1994; Jorstad et al. 2001; Kovalev et al. 2009; Sikora et al. 2009; Abdo et al. 2010). It is unclear for 3C 120 that  $R_\gamma \lesssim R_{\text{BLR}}$  or  $R_\gamma > R_{\text{BLR}}$ , which will significantly influence the gamma-ray spectrum produced in the EC processes. The locations of gamma-ray-emitting regions relative to the BLRs are still an open and controversial issue in the researches on blazars. There are three options for the issue. The first option is that  $R_\gamma \lesssim R_{\text{BLR}}$  for the powerful blazars (e.g. Ghisellini & Madau 1996; Liu et al. 2008; Bai et al. 2009; Tavecchio & Mazin 2009; Ghisellini et al. 2010). The second one is that  $R_\gamma > R_{\text{BLR}}$  (e.g. Bai & Lee 2001; Lindfors et al. 2005; Sokolov & Marscher 2005; Sikora et al. 2008; Marscher et al. 2010; Zhang et al. 2009, 2010). The third option is that the same source can display both behaviors. That is, most of the time the dissipation region is inside the BLR, but there could be some epochs when the gamma-ray-emitting region drift outside the BLR. The very first idea was advanced in Foschini et al. (2011), and a very clear case with multi-wavelength coverage was recently found by Ghisellini et al. (2013). The gamma-ray light curves and the corresponding broad-line light curves should shed light on this issue.

The chosen parameters are average for the jet, and do not correspond to any of the components identified in Jorstad et al. (2005) and Chatterjee et al. (2009). The jet components will have different orientations and different velocities. This seems to be an issue for the choice of jet parameters in equations (1)–(4). The reverberation mapping model assumes the linear response

of broad emission lines to ionizing continuum. In fact, the line response is not linear. It is most likely that the line and radio emission respond nonlinearly to the events in the central engine. Thus some weaker events in the central engine might not produce the correlative responses in the radio and broad-line variations. Both radio and broad-line emission may have good responses to the strongest events in the central engine, and their relevant outbursts should have good matching. There is a matching between these outbursts in the  $H\beta$  line and 15 GHz light curves sampled densely. However, the overall complexity of the light curves and the jet structure at radio bands may lead to difficulties of cross-identifying individual events in different bands. Thus it is difficult to identify the radio knots and radio outbursts corresponding to the broad-line outbursts. We investigated the correlation and time lag between the radio and broad-line light curves by comparing their profiles and cross-correlating them.

The 15 GHz light curve is observed with the 40 m telescope at the Owens Valley Radio Observatory. The 40 m telescope can not resolve the inner jet on the pc scales. Then the 15 GHz fluxes contain all the emission from the inner jet. It is difficult to identify the component responsible for the 15 GHz outburst. It is not possible to determine the relevant velocities of this component along the jet from the central engine to the emitting site of outburst. Thus the average velocity of primary components rather than trailing features will be a good proxy of the global velocity of component emitting outburst. The viewing angle is the same case as the velocity. The similar choice is accepted for the jet parameters for 3C 273 (see Paper I). There are positive and negative time lags between radio variations and those of broad-lines  $H\alpha$ ,  $H\beta$ , and  $H\gamma$  due to the relative short coverage of these line light curves in 3C 273. The longer ultraviolet line light curves show that these broad-line variations lag the radio variations (see Paper II). Thus the broad-line variations lag the radio variations. A constraint of  $R_\gamma \lesssim 0.40\text{--}2.62$  pc is set by these negative time lags (see Paper I). The gamma-ray flares detected with *Fermi*-LAT set a limit of  $R_\gamma < 1.6$  pc for 3C 273 (Rani et al. 2013). The limit is marginally consistent with that constraint of  $R_\gamma \lesssim 0.40\text{--}2.62$  pc. The acceptance of the average parameters of inner jet is reasonable.

In this paper, we find correlation between the broad-line and radio variations with the ZDCF method and the FR/RSS method, and determine a positive lag for the broad-line radio galaxy 3C 120. The positive lag means that the 15 GHz variations lag the  $H\beta$  line variations. We derive  $\tau_{\text{ob}} = 0.34 \pm 0.01$  yr from the FR/RSS method. This time lag is consistent with that estimated from the ZDCF method. Monte Carlo simulations give the radio-emitting location  $R_{\text{radio}} = 5.24 \pm 0.16$  ly from this time lag, the average parameters of inner jet, and equation (4). It is reasonable to use the average parameters of inner jet in equations (1)–(4). This reasonability is supported by the marginal agreement of our previous constraint of  $R_\gamma \lesssim 0.40\text{--}2.62$  pc with the limit of  $R_\gamma < 1.6$  pc from *Fermi*-LAT observations of gamma-ray flares in 3C 273. The underlying baseline of 15 GHz light curve significantly influences the correlation between broad  $H\beta$  line and 15 GHz variations. The subtraction of this baseline from the 15 GHz light curve can well improve the correlation. The longer  $H\beta$  line light curve well sampled may test the correlation. The existence of this correlation is a key to connect the BLR size with the emitting location of jet, and it is important to the gamma-ray emission of AGNs.

We are grateful to Dr. L. Foschini for constructive comments and suggestions. HTL thanks the National Natural Science Foundation of China (NSFC; Grant 11273052) for financial support. JMB acknowledges the support of the NSFC (Grant 11133006). HTL thanks the financial support of the Youth Innovation Promotion Association, CAS and the project of the Training Programme for the Talents of West Light Foundation, CAS.

## REFERENCES

- Abdo, A. A. et al., 2010, *Nat*, 463, 919
- Alexander, T. 1997, in Maoz D., Sternberg A., Leibowitz E. M., eds, *Astronomical Time Series*. Kluwer, Dordrecht, p. 163
- Arshakian, T. G., León-Tavares, J., Lobanov, A. P., Chavushyan, V. H., Shapovalova, A. I., Burdenkov, A. N., & Zensus, J. A. 2010, *MNRAS*, 401, 1231

- Bai, J. M., & Lee, M. G. 2001, *ApJ*, 558, L19
- Bai, J. M., Liu, H. T., & Ma, L. 2009, *ApJ*, 699, 2002
- Blandford, R. D., & McKee, C. F. 1982, *ApJ*, 255, 419
- Blandford, R. D., & Payne, D. G. 1982, *MNRAS*, 199, 883
- Blandford, R. D., & Rees, M. J. 1978, in *Pittsburgh Conf. on BL Lac Objects*, ed. A. M. Wolfe (Pittsburgh, PA: Univ. Pittsburgh Press), p. 328
- Blandford, R. D., & Znajek, R. 1977, *MNRAS*, 179, 433
- Cao, X. W., & Jiang, R. 1999, *MNRAS*, 307, 802
- Cao, X. W., & Jiang, R. 2001, *MNRAS*, 320, 347
- Chatterjee, R. et al., 2009, *ApJ*, 704, 1689
- Chatterjee, R. et al., 2011, *ApJ*, 734, 43
- Celotti, A., Padovani, P., & Ghisellini, G. 1997, *MNRAS*, 286, 415
- Dermer, C. D., & Schlickeiser, R. 1994, *ApJS*, 90, 945
- Edelson, R. A., & Krolik, J. H. 1988, *ApJ*, 333, 646
- Foschini, L., Ghisellini, G., Tavecchio, F., Bonnoli, G., & Stamerra, A. 2011, *Fermi Symposium proceedings*, eConf C110509 (arXiv:1110.4471)
- Ghisellini, G., & Madau, P. 1996, *MNRAS*, 280, 67
- Ghisellini, G., Tavecchio, F., Foschini, L., Ghirlanda, G., Maraschi, L., & Celotti, A. 2010, *MNRAS*, 402, 497
- Ghisellini, G., Tavecchio, F., Foschini, L., Bonnoli, G., & Tagliaferri, G. 2013, *MNRAS*, 432, L66
- Gómez, J. L., Marscher, A. P., Alberdi, A., Jorstad, S. G., & Agudo, I. 2001, *ApJ*, 561, L161
- Grier, C. J. et al., 2012, *ApJ*, 755, 60
- Jorstad, S. G. et al., 2001, *ApJ*, 556, 738
- Jorstad, S. G. et al., 2005, *AJ*, 130, 1418
- Kaspi, S., & Netzer, H. 1999, *ApJ*, 524, 71
- Kaspi, S., Smith, P. S., Netzer, H., Maoz, D., Jan-nuzi, B. T., & Giveon, U. 2000, *ApJ*, 533, 631
- Kataoka, J. et al., 2011, *ApJ*, 740, 29
- Kovalev, Y. Y. et al., 2009, *ApJ*, 696, L17
- León-Tavares, J., Lobanov, A. P., Chavushyan, V. H., Arshakian, T. G., Doroshenko, V. T., Sergeev, S. G., Efimov, Y. S., & Nazarov, S. V. 2010, *ApJ*, 715, 355
- Lindfors, E. J., Valtaoja, E., & Türler, M. 2005, *A&A*, 440, 845
- Liu, H. T., & Bai, J. M. 2006, *ApJ*, 653, 1089
- Liu, H. T., Bai, J. M., & Ma, L. 2008, *ApJ*, 688, 148
- Liu, H. T., & Bai, J. M. 2010, *ScChG*, 53, s240
- Liu, H. T., Bai, J. M., & Wang, J. M. 2011a, *MNRAS*, 414, 155 (Paper I)
- Liu, H. T., Bai, J. M., Wang, J. M., & Li, S. K. 2011b, *MNRAS*, 418, 90 (Paper II)
- Marscher, A. P., Jorstad, S. G., Gómez, J. L., Aller, M. F., Teräsranta, H., Lister, M. L., & Stirling, A. M. 2002, *Nat*, 417, 625
- Marscher, A. P. et al., 2010, *ApJ*, 710, L126
- Meier, D. L., Koide, S., & Uchida, Y. 2001, *Sci*, 291, 84
- Nuñez, F. P. et al., 2012, *A&A*, 545, A84
- Penrose, R. 1969, *Nuovo Cimento Rivista*, 1, 252
- Peterson, B. M., Wanders, I., Bertram, R., Hunley, J. F., Pogge, R. W., & Wagner, R. M. 1998a, *ApJ*, 501, 82
- Peterson, B. M., Wanders, I., Horne, K., Collier, S., Alexander, T., Kaspi, S., & Maoz, D. 1998b, *PASP*, 110, 660
- Peterson, B. M. et al., 2004, *ApJ*, 613, 682
- Peterson, B. M. et al., 2005, *ApJ*, 632, 799

- Rani, B., Lott, B., Krichbaum, T. P., Fuhrmann, L., & Zensus, J. A. 2013, *A&A*, 557, 71
- Rawlings, S., & Saunders, R. 1991, *Natur.*, 349, 138
- Reimer, A. 2007, *ApJ*, 665, 1023
- Richards, J. L. et al., 2011, *ApJS*, 194, 29
- Sikora, M., Begelman, M. C., & Rees, M. J. 1994, *ApJ*, 421, 153
- Sikora, M., Moderski, R., & Madejski, G. M. 2008, *ApJ*, 675, 71
- Sikora, M., Stawarz, L., Moderski, R., Nalewajko, K., & Madejski, G. M. 2009, *ApJ*, 704, 38
- Sitarek, J., & Bednarek, W. 2008, *MNRAS*, 391, 624
- Sokolov, A., & Marscher, A. P. 2005, *ApJ*, 629, 52
- Tavecchio, F., & Ghisellini, G. 2008, *MNRAS*, 386, 945
- Tavecchio, F., & Mazin, D. 2009, *MNRAS*, 392, L40
- Türler, M., Courvoisier, T. J. L., & Paltani, S. 2000, *A&A*, 361, 850
- Wang, J. M. 2000, *ApJ*, 538, 181
- Wang, J. M., Ho, L. C., & Staubert, R. 2003, *A&A*, 409, 887
- Zhang, J., Bai, J. M., Chen, L., & Liang, E. W. 2010, *ApJ*, 710, 1017
- Zhang, J., Bai, J. M., Chen, L., & Yang, X. 2009, *ApJ*, 701, 423